DOI: http://dx.doi.org/10.22104/jpst.2015.64

Journal of Particle Science and Technology (2015) 1-11

Journal of Particle Science and Technology

J | P | S | T

jpst.irost.ir

Investigating the effects of chemical modification of clay nanoparticles on thermal degradation and mechanical properties of TPU/nanoclay composites

Mostafa Gholami [1], Gity Mir Mohamad Sadeghi [1,2,*]

[1] *Department of Polymer Engineering, Amirkabir University of Technology, Mahshahr Campus, Mahshahr, Iran*

[2] *Department of Polymer Engineering & Color Technology, Amirkabir University of Technology,Tehran, Iran*

HIGHLIGHTS

- The effect of chemical modification of clay nanoparticles on thermal/mechanical properties of TPU/nanoclay composites was studied.
- A good dispersion close to exfoliation in the TPU matrix was obtained for cloisite 30B due to hydrogen bonding between carbonyl groups of TPU chains and OH groups of C30B.
- A high content of the clay nanoparticles leads to disordering of soft and hard segments in the TPU chains.

GRAPHICAL ABSTRACT

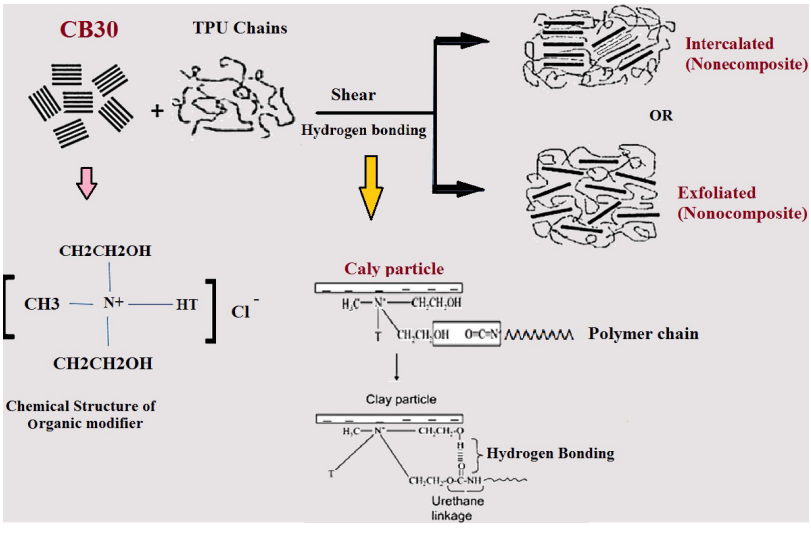

ARTICLE INFO

Article history:
Received 9 October 2014
Received in revised form
2 November 2014
Accepted 6 November 2014

Keywords:
Thermal degradation
Polyurethanes
Nanocomposite
Nanoclay particles
Chemical structure.

ABSTRACT

Thermoplastic polyurethane (TPU)/clay nanocomposites were prepared via a melt-compounding method using ester type TPU and two different modified organoclays (Cloisite 30B and Cloisite 15A) in different contents. The Effects of the chemical structure and content of the nanoclays on the thermal degradation and mechanical properties of TPU were also investigated. The effect of structural modification on dispersion during melt compounding has been studied by XRD and FTIR analysis. Barrier effect formation and thermal stability in both nanocomposites containing different nanoparticle content have been studied. The effect of chemical modification of the nanoparticles on mechanical properties in all contents has been investigated. The XRD results show that better dispersion near the exfoliated structure obtained for cloisite 30B is due to good interaction via hydrogen bonding between the TPU chains and layered silicate. A high content of the nanoparticles leads to disordering of soft and hard segments in the TPU chains, which is confirmed by FTIR. Mechanical properties analysis shows that the TPU/Cloisite 30B nanocomposites have higher modulus and tensile strength as well as elongation at break by the addition of 2% in both cloisite 30B (C30B) and cloisite 15A (C15A) than other contents of nanoclays.

Corresponding author. Tel.: +98 21 664542442; fax: +98 21 66468243.
E-mail address: gsadeghi@aut.ac.ir

1. Introduction

Thermal stability, fire retardancy, mechanical properties like gas barrier properties, and other properties could be improved in polymer nanocomposites [1-4]. PU in different forms (foam, adhesive, coating, elastomer and etc.), is used in various applications. Its great number of applications and combustibility caused it to attract more attention on its degradation and thermal stability [1]. There are a lot of factors that affect polymer nanocomposite properties such as the preparation method (melt compounding, solvent blending and in-situ polymerization), morphology, nanoparticle type and nanoparticle surface treatment methods, crystallinity and molecular weight of the polymer matrix [4]. One of the best preparation methods is melt compounding due to easy processing, high speed and lack of environmental problems compared to the other mentioned methods. Some researchers have studied the preparation of thermoplastic polyurethane (TPU)/ nanoclay composite through the melt compounding method [2, 3, 5, 6, 7]. Pizzatto and his co-workers prepared two kinds of TPU/C30B nanocomposites by melt mixing and bulk polymerization methods. They found that intercalation and better dispersion occurred in melt compounding for TPU/C30B nanocomposite than bulk polymerization due to higher shear viscosity during melt mixing [2]. Dan and his co-workers studied the TPU/Clay nanocomposite via melt mixing, using ester and ether types of TPU and different nanoclays. Good dispersion of nanoclay closes to exfoliation in both ether and ester types of TPU/C30B nanocomposite were found. Nanocomposites based on ether- and ester –TPU/C25A or C15A displayed a partially intercalated structure [3]. Melt compounding quality depends on thermodynamic interactions between polymer chains and layered silicate. This is also affected by the nature of the polymer, loading of layer silicate and structure of the nanoparticles surface treatment. The method was represented by Vaia and his coworkers for the first time in 1993 [8], in which polymer and organically treated clay are heated up to the melting point of the polymer and mixed together by compounding equipment such as extruder or mixing head [4]. As shown in Fig. 1, the morphology of clay-polymer nanocomposites are classified into a) un mixed b) intercalated c) exfoliated. The most favorable morphologies is exfoliated due to its unique final properties.

In this study we used an ester type polyurethane and two kinds of layered silicates (Cloisite15A and Cloisite30B) to prepare the TPU/nanoclay micro- or nanocomposites via a melt-compounding method and attempted to clarify the effect of the chemical structure of the nanoclays type on thermal stability and mechanical properties of the TPU nanocomposites.

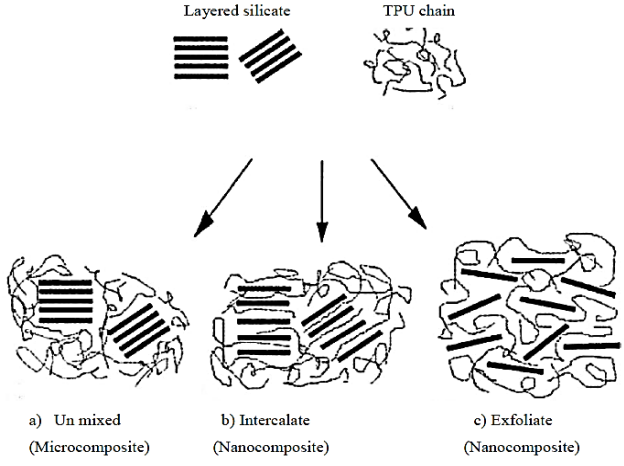

Fig. 1. Polymer /layered silicate structures [9].

2. Experimental

2.1. Materials

The polyester base thermoplastic elastomer polyurethane (TPU Laripur 7025) with specific gravity of 1.18 g/cm^3 and hardness of 70 Shore A was used as a matrix. Cloisite15A is a natural montmorillonite modified with a quaternary ammonium salt with density of 1.66 g/cm^3, d_{001} = 31.50 Å, cation exchange capacity (CEC) of 1.25 meq/g with dimethyl dehydrogenated tallow quaternary ammonium modifier (2M2HT) of tallow composition as ~ 65%C18; ~ 30~ %C16; ~ 5%C14. Cloisite30B is a natural montmorillonite modified with a quaternary ammonium salt, with density of 1.98 g/cm^3, d_{001} = 18.50 Å, CEC of 0.92 meq/g with methyl, tallow, bis-2-hydroxyethyl, quaternary ammonium modifier (MT2 EtOH) of tallow composition as ~ 65%C18; ~ 30~%C16; ~ 5%C14, both purchased from southern clay company.

2.2. Preparation of nanocomposites

The polymer nanocomposites based on TPU, C15A and C30B were prepared by melt compounding technique using Brabender series 30/50 EHT at 185 ^{o}C with a rotor speed of 120 rpm and mixing duration time of 10 min. Different amounts of C30B and C15A nanoclays (2, 4, 6 wt%) were added to the TPU matrix. Before being mixed, the nanoclays were both

dried in a vacuum oven for evaporation of moisture content at 80 °C for 12h and TPU at 80 °C for 4 h. TPU and its nanocomposite sheets (prepared by compression molding) were coded as PU, PU2A, PU4A, PU6A, and PU2B, PU4B, PU6B which demonstrates pure TPU, TPU containing 2, 4, 6 wt % of C15A and TPU containing 2, 4, 6 wt. % of C30B, respectively.

2.3. Characterization techniques

2.3.1. X-ray analysis

X-ray diffraction (XRD) experiments were performed directly on the samples using a Netherland Philips XPert MPD diffractometer (40 kV, 40 mA) with a CO (λ=1.79 Å) irradiation at the rate of 2 °C/min in the range of 1-12°.

2.3.2. Thermal analysis

Thermal gravimetric analyses (TGA and DTG) were carried out using a BAHR Thermo analysis STA 503 thermogravimetric apparatus at nitrogen atmosphere at a heating rate of 10 °C/min. The scanned temperature range was from 50 to 750 °C.

2.3.3. Tensile properties

Tensile properties of the unfilled TPU and its nanocomposite samples were determined using an Instron mechanical tester (model 5566, USA) at crosshead speed of 50 mm/min. Dumbbells with 0.89 mm thickness, 3 mm width and 10 mm length were punched according to ASTM 412. The measurements were done at room temperature. For each sample at least 3 specimens were tested, and the average value was recorded.

2.3.4. Fourier transform infrared (FTIR) spectroscopy

FTIR spectra of the polyurethane and its nanocomposite thin films were carried out using a BOMEM (Canada) spectrometer. Each sample was scanned 20 times with a resolution setting of 4 cm^{-1}. Spectrums were determined in the range of 400-4000 cm^{-1}.

3. Result and discussion

3.1. Study on interaction of TPU / nanoparticles using XRD analysis

XRD patterns of C30B, PU2B, PU4B, and PU6B samples and their basal spacing are shown in Fig. 2 and Table 1, respectively. As shown in Fig.1 and Table 1, the basal spacing (d_{001}) of C30B increased from 18.46 Å to 46.63 Å, 50.80 Å, and 48.6 Å for PU2B, PU4B, and PU6B, respectively. Increasing the basal spacing of the specimens indicates that the polyurethane molecular chains intercalated and expanded the galleries of C30B in all the above mentioned samples [1- 3].

This is attributed to the driving force for intercalation provided by hydrogen bonding between the polymer chains and the polar groups in the nanoparticles. As shown in Fig. 3, the hydroxyl groups of C30B are capable of forming hydrogen bonds with the carbonyl groups in the TPU chains. It is suggested that the hard segments are attracted to the silicate surface and also the soft segments push the platelets apart to regain their entropy [3, 5].

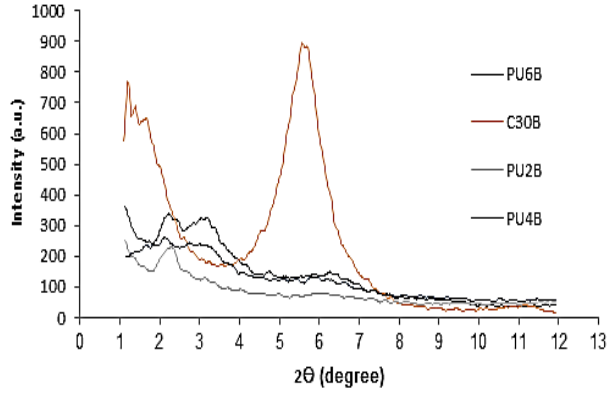

Fig. 2. XRD patterns of C30B and PU2B, PU4B, PU6B nanocomposites.

Table 1.
The basal spacing of TPU/C30B specimens.

	C30B	PU2B	PU4B	PU6B
d_{001}[A°]	18.46	46.63	50.80	48.60
d_{002}[A°]		16.85	35.90	33.66
d_{003}[A°]			17.30	16.35

As shown in Table 1, the peaks of d002-spacing for PU2B, PU4B, and PU6B appeared at 16.85 Å, 35.90 Å, and 33.66 Å, respectively. These peaks are probably due to the presence of nanoclay tactoids in the nanocomposites [2]. According to Table 1, d003-spacing as 17.30 Å and 16.35 Å for PU4B and PU6B respectively, are due to the excess amount of nanoclay in these specimens compared to the PU2B, and also to the poor dispersion in these nanocomposites [2, 10]. As reported by Pizzatto and co-workers [2], for TPU/C30B prepared by melt compounding using the addition of 1 and 3 wt%. nanoclay, only a shoulder has been shown, due to a few nanoclay tactoids, and a peak for 10 wt% of C30B was also due to an excess amount of nano

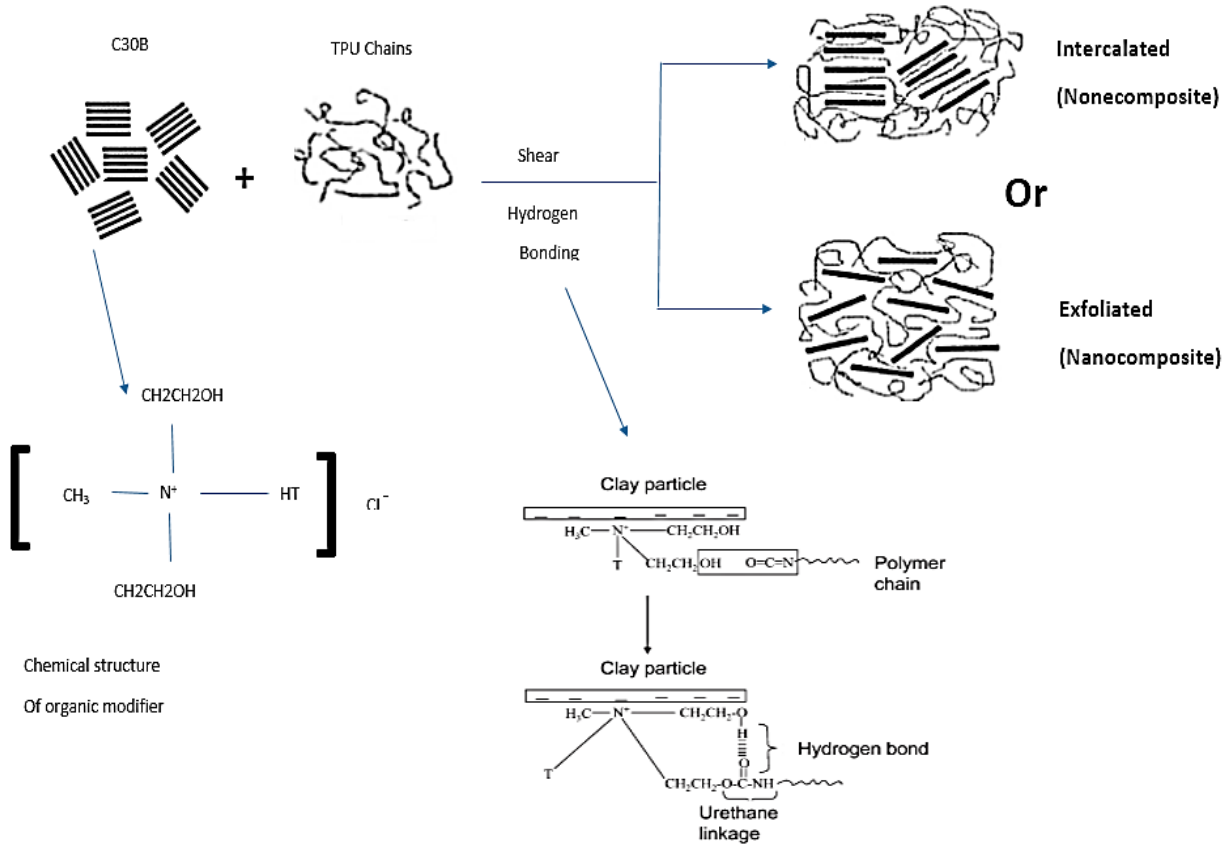

Fig. 3. Increasing of d-spacing by shear and hydrogen bonding between C30B particles and TPU chains.

clay. Furthermore, in two other works, poor dispersion with an increase of nanoclay content in the polymer matrix has been observed [2].

The XRD patterns of C15A, PU2A, PU4A, and PU6A and their basal spacings are shown in Fig. 4 and Table 2, respectively. The basal spacing (d001) of C15A increases from 31.40 Å to 34.70 Å, 34.20 Å, and 35.56 Å in PU2A, PU4A, and PU6A, respectively. In these specimens, increasing the galleries of C15A, about 4 Å, indicates a very poor dispersion of the nanoclay layers in the TPU matrices, which resulted in the molecular chains of TPU not intercalating the galleries of C15A. This is because of the low interaction between C15A and TPU, so we probably have microcomposites in these specimens because the 8 µm particles of C15A cannot change to more than 1 million platelets as shown in Fig. 5 [2, 4].

As shown in Table 2, d_{002} and d_{003} for TPU/C15A specimens are attributed to more stacks and tactoids compared to the TPU/C30B specimens. The 11.50 Å extra peak of d_{004} for PU6A compared to the PU2A and PU4A is due to the presence of an excess amount of nanoparticles in these specimens. Finally, comparing C30B and C15A shows better dispersion than that obtained for C30B in TPU matrices. This phenomenonis due to good interaction between the layers of C30B and the chains of TPU. As reported by Dan and co-workers [3], better dispersion was observed for C30B in the TPU matrix by melt mixing compared to the C15A due to good interaction between hydroxyl groups of C30B and carbonyl groups in the used ether-ester type TPU [3].

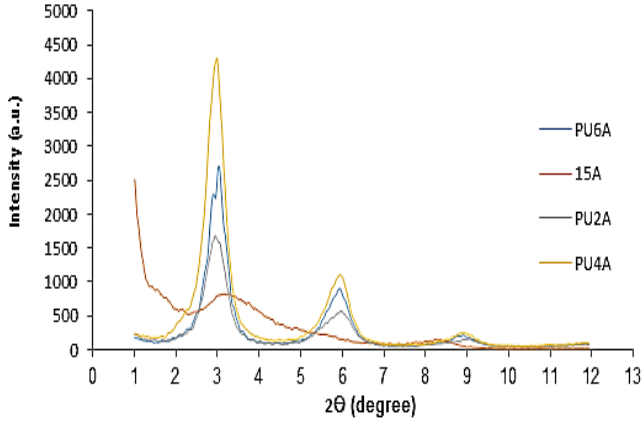

Fig. 4. XRD patterns of C15A and PU2A, PU4A and PU6A nanocomposites.

Table 2.
The basal spacing of TPU/C15A specimens.

	C15A	PU2A	PU4A	PU6A
d_{001}[A°]	31.40	34.70	34.20	35.56
d_{002}[A°]	12.33	17.16	17.19	3384
d_{003}[A°]		11.32	11.60	17.29
d_{004}[A°]				11.50

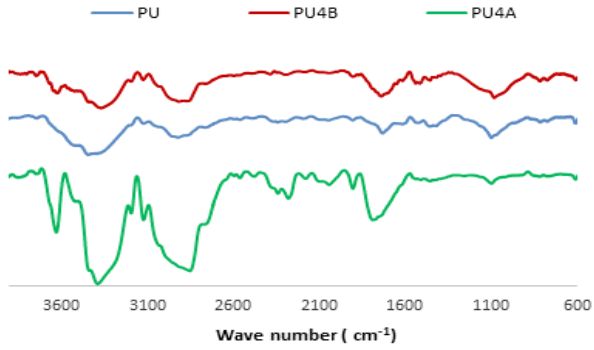

Fig. 6. FTIR spectra of PU, PU4B and PU4A specimens.

3.2. FTIR analysis

The infrared spectroscopic technique is a useful tool to determine chemical changes that perhaps happen during melt compounding [11]. Two cardinal regions that are important in this study are –NH and –C=O peaks. Investigation of –NH and carbonyl peaks in the FTIR spectra was performed to obtain useful information about the interaction between clay particles and TPU chains [12]. The FTIR spectra of pure PU, PU4B and PU4A are shown in Fig.6. As shown in Figure 6 for pure TPU, the peak at around 3452 cm^{-1} is due to free –NH, and the peaks at around 2925 cm^{-1}, 2874 cm^{-1} and 2763 cm^{-1} are due to C-H asymmetric stretching, C-H symmetric stretching and C-H in CH_2-O stretching mode, respectively. The peaks at around 1730 cm^{-1} and 1618 cm^{-1} are due to stretching mode

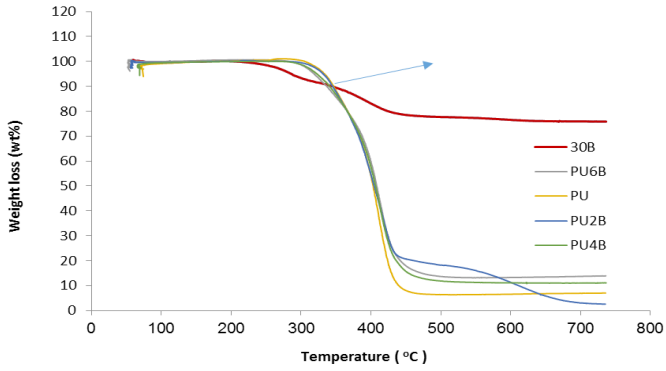

Fig. 7. TGA Thermograms of PU, C30B and PU2B, PU4B, PU6B nanocomposites.

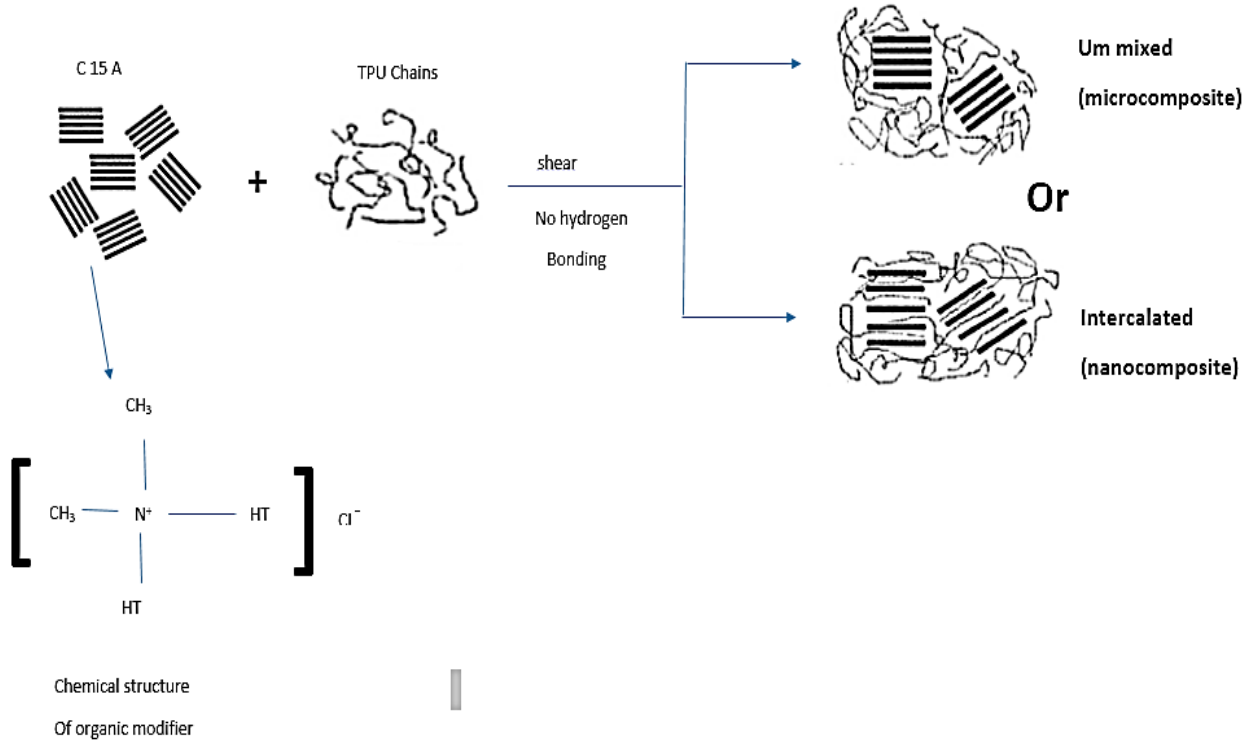

Fig. 5. Increasing of d-spacing C15A by shear in TPU/C15A.

of C=O, free urethane carbonyl and stretching mode of C=O, H-bonded ordered urea carbonyl, respectively. The peaks at around 1451 cm^{-1} and 1411 cm^{-1} are due to in-plane bending of C-H in CH_2 and stretching mode of C-C in the aromatic ring, respectively [3, 12 - 15]. As shown in Fig. 6, the FTIR spectrum of PU4B shows a peak at around 1735 cm^{-1} that is due to the stretching mode of C=O in free urethane carbonyl and there is no peak for H-bonded ordered urea carbonyl at around 1618 cm^{-1}, because of disordering by dispersion of nanoclay. The peak at around 3371 cm^{-1} is due to the stretching mode of N-H free and the peak at around 3624 cm^{-1} is due to –OH stretching modes of Al-OH of MMT [16]. As shown in Fig. 6, the FTIR spectrum of PU4A shows a peak at around 1791 cm^{-1} that is due to the C=O stretching mode of free urethane carbonyl and there is no peak for H-bonded ordered urea carbonyl at around 1618 cm^{-1}, because of disordering by dispersion of nanoclay. The peak at around 3391 cm^{-1} is due to stretching modes of N-H free and the peak at around 3629 cm^{-1} is due to –OH stretching modes of Al-OH of MMT [16].

3.3. Thermal degradation analysis

TGA and DTGA analysis of TPU, C30B and their nanocomposites are shown in Figs. 7 and 8, respectively. The temperature at 5% and 50% weight loss (T5% and T50%), degradation steps, temperature range of each step and weight loss of each step for TPU, C30B and prepared nanocomposites are shown in Table 3. Also, char residue at 450, 500, 600, and 700 oC. Polyurethanes are almost thermally unstable polymers and their degradation depends on their structures. Polyurethanes degradation usually starts with decomposition of hard segment, dissociation of the urethane bond, carbon dioxide and isocyanate evaporation [14]. As shown in Figs.7 and 8, the degradation patterns of TPU and its nanocomposites are similar. Two steps of weight loss for all specimens are seen except for PU2B. It is generally believed that the addition of clays (or any inorganic material) into the polymeric matrices can improve their thermal stability. Dispersed silicate layers ban the penetration volatile degradation products out of the materials by the "barrier effect" which delays the release of degradation products in comparison to the pure polymer [7, 17 - 19]. Generally, all of the organically modified montmorillonites decompose in similar patterns. They show three to four DTGA peaks, a sharp peak at about 250 oC and three to four DTGA peaks in the range of 300 to 400 oC. For the Cloisite groups of clay, releasing water begins at about 40 oC and continues to 200 oC. At about 200 to 500 oC, the organic constituent in the organically modified layered silicate begins to decompose, as some other researchers [1, 7] mentioned in literature. As shown in Fig. 9, thermal degradation of OMT begins at about 200 oC, and continues according to the Hoffman degradation mechanism [9]. It occurs in the presence of a main anion, such as hydroxide, which expels hydrogen from an alkyl group, yielding an olefin and a free amine. Subsequently, the proton generated from the elimination reaction moves to the clay surface and forms a Bronsted acidic site. When the organic modifier is decomposed completely, it can be considered

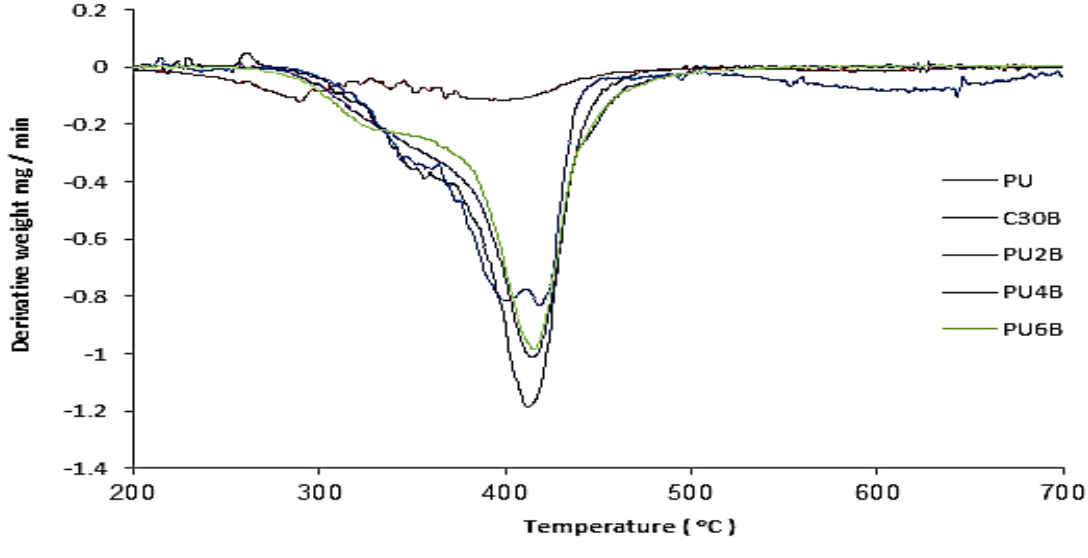

Fig. 8. DTGA Thermograms of PU, C30B and PU2B, PU4B, PU6B nanocomposites.

as acid activated clay and has direct interface with the remaining polymer chains. The amount of acidic sites are related to the cationic exchange capacity of MMT. Clays in the acid forms are famous for making the hydrocarbon cracking and/or hydrocarbon aromatization easy, depending on the silicate structure and acidity [1, 9].

more char residue than pure TPU is due to the "barrier effect" which means that the silicate layers hinder the permeability of volatile degradation products out of the TPU matrix and also chars residue of the mineral material in MMT.

TGA and DTGA patterns of TPU, C15A, and their nanocomposites are shown in Fig. 10 and 11, respectively.

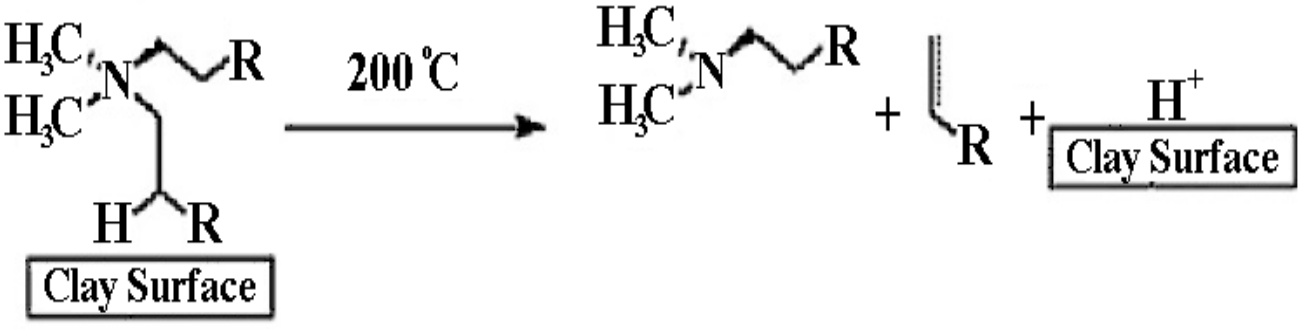

Fig. 9. Hoffman elimination reaction of alkyl ammonium organic treatment [9].

As illustrated in Table 3, C30B does not improve thermal stability of TPU at the beginning of the degradation process (T5%) and as mentioned above it is because of the degradation of nanoclay that occurs in the lower temperatures and makes the degradation of TPU easy, at T5%. Among these nanocomposites, PU2B has better thermal stability than PU4B and PU6B at T5%, is probably due to the lower amount of nanoclay in this specimen, yielding less acidic sites than the others. However Pattanayak and co-workers [13] showed an improvement in thermal stability at T5% with increasing C30B to the TPU polyether type. These differences are probably due to the presence of carbonyl groups in the TPU/ester type (present work) that have more hydrogen bonding and good interaction with C30B than TPU/ether type, resulting in a greater effect of the acidic site on TPU/ester chains at T5%.

As shown in Table 3, the addition of C30B caused improvement in thermal stability of TPU at 50% weight loss (T50%). According to Table 3, it happens in the second step of the TPU degradation process. In the second step, dispersed silicate layers delay the release of volatile degradation products from the nanocomposite [18]. A comparison of the results shows that thermal stability of PU6B is higher than PU4B and PU4B is higher than PU2B and it is clear that a greater amount of nanoclay makes thermal stability in the nanocomposite higher at T50%. As shown in Fig. 7 and Table 3, generally the nanocomposites having

The temperature at 5% and 50% weight loss (T5% and T50%), degradation steps, temperature range of each step and weight loss of each step for TPU, C15A, and their nanocomposites are shown in Table 4, and also char residue at 450, 500, 600, and 700 oC. As mentioned before, degradation of C30B and C15A are similar and they occur according to the Hoffman mechanism. As illustrated in Fig. 10 and Table 4, C15A caused TPU/C15A nanocomposites to have less thermal stability than TPU at (T5%) in all specimens. This is due to the formed acidic sites in C15A that help the degradation of TPU at the first step. T50% does not have any improvement which is probably due to the low nanoclay dispersion and low interaction between layered silicate of C15A and TPU as mentioned before in the XRD analysis section. However Barick and co-worker [7] observed improvements in thermal stability for polyether-based TPU/C15A nanocomposites and mentioned that degradation rates of nanocomposites became slower compared to the TPU due to the layered silicate that could prevent heat spread and limits further degradation [7]. Comparing the results in Table 3 and Table 4 shows that C15A lead to better thermal stability than C30B/TPU at T5% which is due to the lower effect of acidic sites of C15A rather than C30B due to less hydrogen bonding interaction between C15A and TPU chains. However for T50%, C30B gives better thermal stability to TPU than C15A. This is because of the good dispersion of layers as well as good

interaction between silicate layers of C30B and TPU chains as mentioned before in XRD analysis. however Cervantes and co-workers, [17] in their study for PU/Na+, C15A, and C30B nanocomposites observed that just TPU/C15A showed an increase in thermal stability with an increase in C15A content and mentioned that this occurred due to good interaction between clay and TPU [17]. As shown in Table 4, in the first step, the weight loss of PU2A, PU4A, and PU6A is more than pure TPU which is due to degradation of C15A that occurs in lower temperatures. In the second step, the existence of C15A in TPU makes nanocomposites

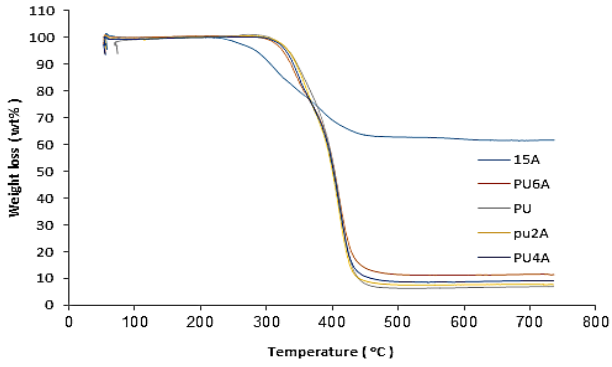

Fig. 10. TGA thermogram of PU, C15AB and PU2A, PU4A, PU6A of specimens.

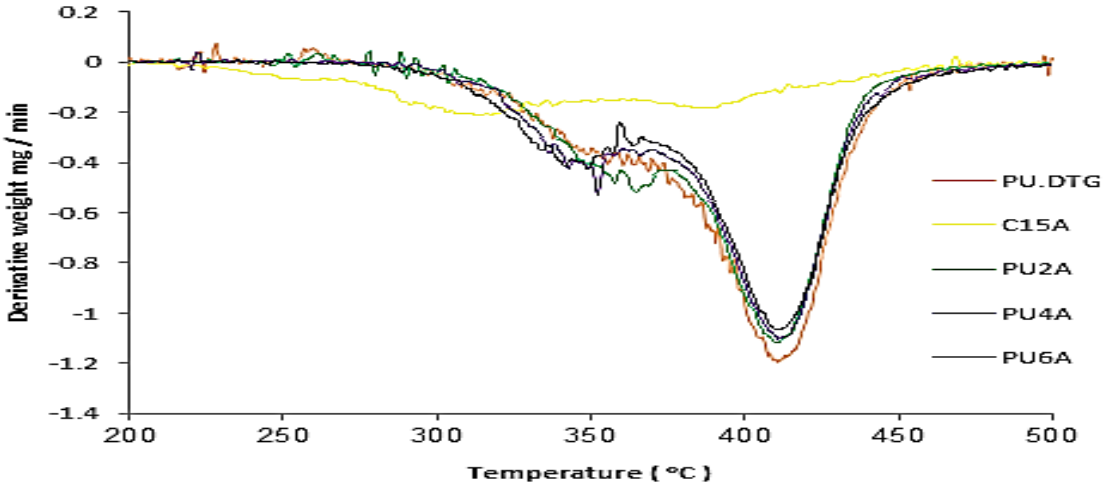

Fig. 11. DTGA thermogram of PU, C15A and PU2A, PU4A, PU6A specimens.

Table 3.
Some thermal properties of TPU/C30B specimens.

	PU	C30B	PU2B	PU4B	PU6B
$T_{5\%}$(°C)	334	286.30	331.50	322	319
$T_{50\%}$(°C)	403		404.60	406.60	408
1t step range (°C)	280-365	180-310	280-355	270-370	262-375
Weight loss%	20	8	15	22.10	24
2t step range (°C)	365-480	325-495	355-404	370-510	375-510
Weight loss%	73	14.70	35.40	66.30	62.50
3t step range (°C)		525-630	404-500		
Weight loss%		1.20	32		
4t step range (°C)			520-680		
Weight loss%			14		
Char residue at 450 (°C)	8	78.50	20.70	15.60	17.90
Char residue at 500 (°C)	6.35	77.68	18.20	11.80	13.60
Char residue at 600 (°C)	6.50	76.50	11.30	11	13.24
Char residue at 700 (°C)	6.90	75.90	3	11	13.60

Table. 4.
Some thermal properties of TPU/C15A specimens.

	PU	C15A	PU2A	PU4A	PU6A
$T_{5\%}$(°C)	334	284.75	333.10	329.90	324.50
$T_{50\%}$(°C)	403		400	401.60	403.50
1t step range (°C)	280-365	195-260	285-370	285-360	270-360
Weight loss%	20	2.50	26	21	23.50
2t step range (°C)	365-480	260-350	370-470	370--485	370-495
Weight loss%	73	18	66	69.90	74.80
3t step range (°C)		350-500			
Weight loss%		16.80			
4t step range (°C)		550-650			
Weight loss%		1.20			
Char residue at 450 (°C)	8	63.50	9.02	10.80	13.90
Char residue at 500 (°C)	6.35	62.78	7.60	8.70	11.40
Char residue at 600 (°C)	6.50	61.98	7.60	8.70	11.20
Char residue at 700 (°C)	6.90	61.60	7.70	9.10	11.50

have less weight loss than pure TPU except for PU6A. This is due to a greater amount of nanoclay and weak dispersion of layers in PU6A as mentioned before in the XRD analysis section. As shown in Table 4, the addition of C15A into TPUs leads to having more char residue for all specimens rather than pure TPU. Comparing Tables 3 and 4 shows that the char residue for TPU/C30B nanocomposites is more than TPU/C15A nanocomposites which is due to good dispersion for C30B and obviously better obtained interaction between TPU and C30B as mentioned before.

3.4. Tensile properties

Stress-strain curves of unfilled TPU and its C30B, C15A nanocomposites are shown in Fig. 12 and 13, respectively. Values of modulus, tensile strength, and elongation at break of specimens are shown in Table 5.

Generally, the addition of nanoparticles has two different effects on tensile properties of TPU: a) High modulus of clay nanoparticles leads to increasing the modulus of TPU. b) The nanoparticles simultaneously interfere with the formation of hard segment domains and cause a decrease in modulus [20]. Tensile properties of the nanocomposites are the result of balance between these two effects. As Table 5 shows, the addition of C30B and C15A to TPU caused the modulus to increase compared to the pure TPU in all percentages of strain and amounts of nanoclay except for PU4B, PU2A, and PU6A at 50% strain. This is due to the high modulus of nanoclay, and an increase in the modulus for polymeric composites even without noticeable interfacial attraction between polymer matrices and inorganic fillers can occur. Among the values of the modulus, the best improvement is obtained for PU2B. This is because of the good dispersion of C30B in TPU and good interaction between the layered silicate of C30B and the TPU chains as mentioned before. As shown in Table 5, the addition of C30B and C15A to TPU caused an increase in tensile strength and elongation at the break just for PU2B

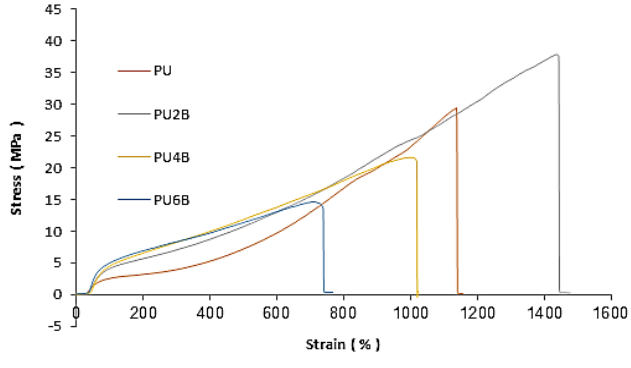

Fig. 12. Tensile stress versus strain for the PU, PU2B, PU4B, and PU6B specimens.

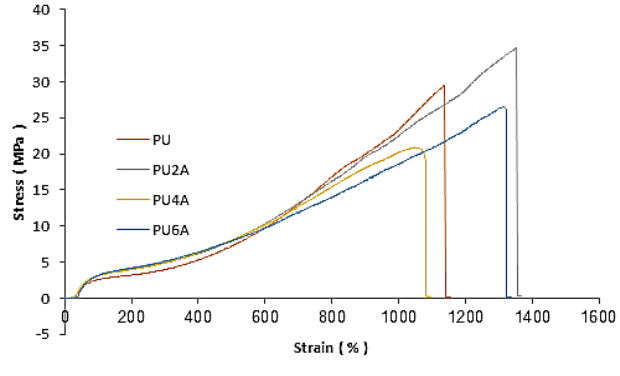

Fig. 13. Tensile stress versus strain for the PU, PU2A, PU4A, and PU6A specimens.

Table. 5.
The values of modulus, tensile strength and elongation at break of specimens.

	Modulus at 50% strain(MPa)	Modulus at 100% strain(MPa)	Modulus at 300% strain(MPa)	Modulus at 600% strain(MPa)	Tensile strength (MPa)	Elongation at break (%)
PU	2.78	2.54	1.13	1.60	29.44	1136
PU2B	3.40	4.11	2.35	2.17	37.50	1443
PU4B	2.36	4.53	2.75	2.29	21.64	1003
PU6B	4.50	5.03	2.78	2.18	14.60	715
PU2A	2.46	3.10	1.63	1.72	34.70	1353
PU4A	3.46	3.12	1.63	1.70	19.20	1080
PU6A	2.46	3.12	1.70	1.61	26.20	1321

and PU2A. Also, PU2B is better than PU2A because of the good interaction provided by hydrogen bonding between the chains of TPU and nanoparticles of C30B. However for 4 and 6% of C30B and C15A, the addition of nanoclay does not improve the tensile strength and elongation at the break because of the poor dispersion and the existence of agglomerated nanoclay tactoids. These nanoclay tactoids are not capable of aligning in the strain direction and caused concentrated tensile stresses between the polymer and filler instead of suitable shear stresses, resulting in void formation and reduced tensile strength and elongation at break as other researchers reported in the literature [2, 3, 5, 13, 20].

Dan and co-workers [3] showed that increasing C30B 10%wt resulted in significant improvement in the modulus and it was better than C15A [3]. Also, Finnigan and co-workers [5] observed improvement in the modulus with an increase of C30B, and good dispersion of C30B in the TPU matrix caused a decrease in elongation at break with an increase of C30B [5]. Pattanayak and co-workers [8] showed that the modulus, tensile strength, and elongation at break generally increase with an increase of nanoclay content [13].

4. Conclusions

The ester type TPU/clay nanocomposites were prepared by a melt-compounding method using various contents of clay nanoparticles having different structural modifications. XRD and FTIR confirm a good dispersion of C30B close to exfoliation in the TPU matrix due to hydrogen bonding between the carbonyl groups of the TPU chains and the hydroxyl groups of C30B. More interaction between TPU chains and layers of C30B results in better dispersion of C30B into the TPU matrix. This phenomenon caused the barrier effect formation which increases thermal stability and char residue of TPU/C30B nanocomposites at T50% in all contents. The addition of C30B and C15A in the TPU matrix caused the modulus to improve in all percentages of strain and nanoclay contents except for 50% strain. Low contents of both nanoclays into the TPU matrix, shows higher tensile strength and elongation at break than other nanocomposites. However a high content of the nanoparticles leads to disordering of soft and hard segments in TPU chains, which is confirmed by FTIR.

References

[1] L. Song, Y. Hu, Y. Tang, R. Zhang, Z. Chen, W. Fan, Study on the properties of flame retardant polyurethane/organo clay nanocomposite, Polym. Degrad. Stab. 87 (2005) 111-116.

[2] L. Pizzatto, A. Lizot, R. Fiorio, C. Amorim, G. Machado, M. Giovane La, A. Zattera, J. Crespo, Synthesis and characterization of thermoplastic polyurethane/nanoclay composite, Mater. Sci. Eng. 29 (2009) 474-478.

[3] C. Dan, M. Lee, Y. Kim, B. Min, J. Kim, Effect of clay modifiers on the morphology and physical properties of thermoplastic polyurethane/clay nanocomposite, Polym. 47 (2006) 6718-6730.

[4] J. H. Koo, Polymer Nanocomposites: Processing, Characterization, and Applications , McGraw-Hill, New York, 2006.

[5] B. Finnigan, D. Martin, P. Halley, R. Truss, K. Campbell, Morphology and properties of thermoplastic polyurethane nanocomposite incorporating hydrophilic layered silicates, Polymer 45 (2004) 2249-2260.

[6] X. Meng, X. Du, Z. Wang, W. Bi, T. Tang, The investigation of exfoliation process of organic modified montmorillonites in thermoplastic polyurethane with different molecular weights, Compos. Sci. Technal. 68 (2008) 1815-1821.

[7] A. Barick, D. Tripathy, Thermal and dynamic mechanical characterization of thermoplastic polyurethane/organoclay nanocomposites prepared by melt compounding, Mater. Sci. Eng. 527 (2010) 812-823.

[8] R. A. Vaia, H. Ishii, E. P. Giannelis, Synthesis and properties of two dimensional nanostructures by direct intercalation of polymer melts in layered silicates, Chem. Mater. 5 (1993) 1694-1696.

[9] P. Kiliaris, C. Papaspyrides, Polymer/Layered silicate (clay) nanocomposites: An overview of flame retardancy, Prog. Polym. Sci. 35 (2010) 902-958.

[10] J. S. MA, S. F. zhang, Z. N. Qi, synthesis and characterization of elastomeric polyurethane/clay nanocomposites, Appl. Polym. Sci. 82 (2001) 1444-1448.

[11] M. Jalili, S. Moradian, Deterministic performance parameters for an automotive polyurethane clearcoat loaded with hydrophilic or hydrophobic nano-silica, Prog. Org. Coat. 66 (2009) 359-366.

[12] W. Kim, D. Chang, J. Kim, Effect of Length of hydroxyalkyl group in the clay mdifier on the properties of thermoplastic polyurethane/clay nanocomposites, Appl. Polym. Sci. 110 (2008) 3209-3216.

[13] A. Pattanayak, S. Jana, Thermoplastic polyurethane nanocomposites of reactive silicate clays: effects of soft segments on properties, Polymer 46 (2005) 5183-5193.

[14] G. M. M. Sadeghi, M. Aslzadeh, M. Abdouss, Synthesis and characterization of BHETA based new polyurethanes, Mat.-wiss. u. Werkstofftech. 41 (2010) 682-688.

[15] R. Shamsi, M. Abdous, G. M. M. sadeghi, F. Afshar, Synthesis and characterization of novel polyurethanes based on aminolysis of poly (ethylene terephthalate) wastes, and evaluation of their thermal and mechanical properties, Polym. Int. 58 (2009) 22-30.

[16] S. Semenzato, A. Lorenzetti, M. Modesti, E. Ugel, D. Hrelja, S. Besco, R. Michelin, A. Sassi, G. Facchin, A norel phosphorus polyurethane foam/montmorillonites nanocomposite: preparation, characterization and thermal behavior, Appl. Clay Sci. 44 (2009) 35-42.

[17] J. Cervantes, M. Espinosa, J. Cauich-Rodriguez, A. Avila-Ortega, H. Vazquez-Torres, A. Marcos-Fernandez, J. Roman, TGA/FTIR Studies of segmented aliphatic polyurethanes and their nanocomposites prepared with commercial montmorillonites, Polym. Degrad. Stab. 94 (2009) 1666-1677.

[18] M. Berta, C. Lindsay, G. Pans, G. Camino, Effect of chemical structure on combustion and thermal behavior of polyurethane elastomer layered silicate nanicomposites, Polym. Degrad. Stab. 91(2006)1179-1191.

[19] J. Seyfi, I. Hejazi, G. M. M. Sadeghi, M. Davachi, S. Ghanbar, Thermal degradation and crystallization Behavior of Blend-Based nanocomposites: Role of clay network formation, Appl. Polym. Sci. 123 (2011) 2492-2499.

[20] T. Fattahi, G. M. M. Sadeghi, F. Dadashian, H. Ebrahimi, From cellulosic waste to nanocomposite. Part 2: synthesis and characterization of polyurethane/cellulose nanocomposites, Mater. Sci. 48 (2013) 7283-7293.